Organization of the Yeast Zip1 Protein within the Central Region of the Synaptonemal Complex

Hengjiang Dong*§ and G. Shirleen Roeder*‡§

*Department of Molecular, Cellular and Developmental Biology, ‡Department of Genetics, and §Howard Hughes Medical Institute, Yale University, New Haven, Connecticut 06520-8103

Abstract. The yeast Zip1 protein is a component of the central region of the synaptonemal complex (SC). Zip1 is predicted to form an α-helical coiled coil, flanked by globular domains at the NH_2 and COOH termini. Immunogold labeling with domain-specific anti–Zip1 antibodies demonstrates that the NH_2-terminal domain of Zip1 is located in the middle of the central region of the SC, whereas the COOH-terminal domain is embedded in the lateral elements of the complex. Previous studies have shown that overproduction of Zip1 results in the assembly of two types of aggregates, polycomplexes and networks, that are unassociated with chromatin. Our epitope mapping data indicate that the organization of Zip1 within polycomplexes is similar to that of the SC, whereas the organization of Zip1 within networks is fundamentally different. Zip1 protein purified from bacteria assembles into dimers in vitro, and electron microscopic analysis demonstrates that the two monomers within a dimer are arranged in parallel and in register. Together, these results suggest that two Zip1 dimers, lying head-to-head, span the width of the SC.

Key words: *Saccharomyces cerevisiae* • meiosis • chromosome synapsis • transverse filament • polycomplex

Introduction

Meiosis is a special type of cell division that produces four haploid products from a single diploid cell. This reduction in chromosome number occurs at the first meiotic division, when homologous chromosomes segregate to opposite poles of the spindle apparatus. Proper reductional chromosome segregation depends on a complex series of interactions between homologues, including formation of the synaptonemal complex (SC)[1] (Roeder, 1997).

The SC is an elaborate proteinaceous structure that holds homologous chromosomes close together along their lengths during the pachytene stage of meiotic prophase (von Wettstein et al., 1984; Heyting, 1996; Roeder, 1997). Each SC consists of two lateral elements, corresponding to the protein backbones of the individual chromosomes within the complex. Lateral elements are referred to as axial elements before their incorporation into mature SC. The central region lies between the two lateral elements and consists of two distinctive substructures. The central element lies parallel to and equidistant between the two lateral elements, whereas transverse filaments lie perpendicular to the long axis of the complex. Some transverse filaments appear to span the full width of the SC, bridging the space between the two lateral elements; other transverse filaments are shorter and connect a single lateral element to the central element (Schmekel and Daneholt, 1995). The structure and dimensions of the SC are highly conserved across species (von Wettstein et al., 1984).

Structural components of the SC have been identified in a number of organisms (Heyting, 1996; Roeder, 1997). One of the best characterized is the Zip1 protein of *Saccharomyces cerevisiae*. Several observations indicate that Zip1 is a building block of the transverse filaments of the yeast SC (Sym et al., 1993; Sym and Roeder, 1995; Tung and Roeder, 1998). In the *zip1* null mutant, axial elements are fully developed and homologously paired, but they are not intimately synapsed. Anti-Zip1 antibodies localize continuously along the lengths of synapsed meiotic chromosomes, but not to unsynapsed axial elements. The sequence of the Zip1 protein predicts a long stretch of α-helical coiled coil (Steinert and Roop, 1988; Lupas et al., 1991) near the middle of the protein. Based on this similarity to myosin and intermediate filament proteins, Zip1 has been postulated to form a rod-shaped homodimer flanked by globular domains (Sym et al., 1993; Sym and Roeder, 1995). Mutations that increase or decrease the length of

Address correspondence to G. Shirleen Roeder, Department of Molecular, Cellular and Developmental Biology, Howard Hughes Medical Institute, Yale University, 219 Prospect Street, P.O. Box 208103, New Haven, CT 06520-8103. Tel.: (203) 432-3501. Fax: (203) 432-3263. E-mail: shirleen.roeder@yale.edu

[1]*Abbreviations used in this paper:* EM, electron microscope; GST, glutathione-S-transferase; SC, synaptonemal complex; 6xHis, hexamer of histidine residues.

the Zip1 coiled coil lead to corresponding alterations in the width of the SC, indicating that the rod-shaped Zip1 molecule lies perpendicular to the long axis of the complex (Sym and Roeder, 1995; Tung and Roeder, 1998). Overproduction of Zip1 induces the formation of two chromatin-free, highly ordered structures, called polycomplexes and networks, that contain large amounts of the Zip1 protein (Sym and Roeder, 1995).

Protein components of the central region of the SC have also been identified in mammals. These include the SCP1 protein of rats and homologues of SCP1 in hamsters (Syn1), mice, and humans (Meuwissen et al., 1992, 1997; Dobson et al., 1994; Liu et al., 1996). Like Zip1, each of these proteins is predicted to form an α-helical coiled coil flanked by globular regions. In addition, these proteins localize specifically to the central region of synapsed meiotic chromosomes. However, in terms of amino acid sequences, the SCP1/Syn1 proteins are no more similar to Zip1 than expected for any two proteins containing coiled coils. Epitope-mapping experiments demonstrate that SCP1 and Syn1 lie perpendicular to the long axis of the complex, with their COOH termini located in the lateral elements and their NH_2 termini positioned at or near the middle of the central region (Dobson et al., 1994; Liu et al., 1996; Schmekel et al., 1996). A similar organization was recently proposed for Zip1 based on genetic and cytological analyses of a series of in-frame deletion mutations affecting the Zip1 protein (Tung and Roeder, 1998).

To define precisely the organization of Zip1 within the SC, we have mapped different domains of the protein by immunoelectron microscopy using domain-specific anti–Zip1 antibodies. The results indicate that the NH_2-terminal domain of Zip1 lies in the middle of the central region of the SC, whereas the COOH-terminal domain is anchored to the lateral elements. These data suggest that two Zip1 dimers, lying head-to-head, span the width of the SC. Thus, the organization of Zip1 is similar to that proposed for the SCP1/Syn1 proteins. Although it is generally assumed that Zip1 (and SCP1/Syn1) form homodimers, this has not been directly demonstrated. Here, we report that Zip1 protein purified from bacteria forms homodimers in vitro. Analysis of these dimers in the electron microscope (EM) demonstrates that the two Zip1 monomers within a dimer are organized in parallel and in register.

Materials and Methods

Generation and Purification of Antibodies

To generate antibodies specific for different domains of Zip1, nonoverlapping fragments of the *ZIP1* gene were fused in-frame to the glutathione-S-transferase (*GST*) gene in pGEX-KG (Guan and Dixon, 1991) (see Fig. 1). pHD100 (encoding Zip1-coil) was constructed by subcloning the HincII fragment encoding amino acids 511–823 from pTP29 (Tung and Roeder, 1998) into the unique SmaI site of pGEX-KG. pHD102 (encoding Zip1-N) was made by inserting the BamHI fragment encoding amino acids 20–139 into the BamHI site of pGEX-KG. The HincII-XbaI fragment containing codons 824–875 plus ~250 nucleotides of downstream sequence was cloned into the SmaI-XbaI sites of pGEX-KG, to generate pHD103 (encoding Zip1-C).

pHD100, pHD102, and pHD103 were transformed into *Escherichia coli* XL1-Blue (Sambrook et al., 1989), and the three GST-Zip1 fusion proteins were overproduced and purified according to the procedure of Guan and Dixon (1991). All three GST-Zip1 fusion proteins were sent to the Pocono Rabbit Farm and Laboratory for immunization of rabbits. In addition, the GST-Zip1-C fusion protein was used to raise antibodies in guinea pigs.

Antibodies were purified from sera in two steps. First, antibodies against GST were removed by passing 2 ml of serum through a glutathione agarose column (4-ml bed volume) coupled to ~2 mg of GST proteins purified from 1 liter of bacterial cells overexpressing the *GST* gene alone (Guan and Dixon, 1991). The flow-through fractions were pooled and applied to a 2-ml Sepharose 4B column coupled to 2 mg of the appropriate GST-Zip1 fusion protein. Proteins were coupled to CNBr-activated Sepharose 4B beads according to the manufacturer's instructions (Pharmacia Biotech). After washing with 20 ml of PBS buffer (Sambrook et al., 1989) containing 1% Triton X-100 and with 20 ml of PBS buffer, the antibody was eluted from the column using a linear pH gradient descending from 6.0 to 3.0 in 0.1 M citric acid. The peak fractions containing antibodies were pooled and concentrated into a total volume of 0.5 ml using Centricon-100. After dialysis against 1 liter of PBS buffer containing 0.02% sodium azide for 6 h, the purified antibodies were aliquoted and stored frozen at −70°C.

Western Blot Analysis

To test the specificity of antibodies, aliquots of the three GST-Zip1 fusion proteins were fractionated on four identical 12% polyacrylamide gels containing SDS (Sambrook et al., 1989). Three gels were blotted onto nitrocellulose filters, whereas one gel was stained with Coomassie brilliant blue R250 (Sambrook et al., 1989). Each blot was probed with one of the affinity-purified anti–Zip1 antibodies. After hybridization with the primary rabbit antibody (1:2,000 dilution), the filters were incubated with the secondary goat anti–rabbit IgG conjugated with alkaline phosphatase (1:200 dilution) (Jackson ImmunoResearch Laboratories). The protein bands were visualized using the CDP-*Star* detection system (Boehringer Mannheim).

Immunogold Labeling

The procedure for preparation of meiotic nuclear spreads (Sym et al., 1993) was modified as follows. First, meiotic chromosomes were surface spread onto plastic-coated slides that had been glow-discharged (Dodson and Echols, 1991). Second, the chromosome spreads were treated with 100 U/ml DNase I for 30 min at room temperature (Smith and Roeder, 1997). The yeast strains used for preparation of chromosome spreads were BR2495 (Rockmill and Roeder, 1990) and a *zip1* null mutant derivative containing the multicopy plasmid pMB185 (*zip1-3XH2*) (Sym and Roeder, 1995). After drying, the plastic film containing chromosome spreads was transferred to 100-mesh nickel grids (Electron Microscopy Sciences). Immunogold labeling was performed by placing each grid on a drop (50 μl) of solution containing the primary anti–Zip1 antibody on a piece of parafilm such that the chromosome spreads were in direct contact with the antibody solution. Grids were incubated with primary antibody in a humid chamber at 4°C overnight. After washing three times for 30 min with PBS buffer containing 0.5% Triton X-100 at room temperature, the grids were incubated with the secondary antibody conjugated to colloidal gold for 5 h at 4°C. After washing another three times, each grid was air dried.

For single labeling, the primary antibodies derived from rabbit were used at 1:200 dilution. The secondary antibody was goat anti–rabbit IgG conjugated to 12-nm colloidal gold used at 1:400 dilution (Jackson ImmunoResearch Laboratories). For double labeling of the SC with different sizes of gold particles, a mixture of rabbit anti–Zip1-N and guinea pig anti–Zip1-C antibodies, each at 1:200 dilution, were used as the primary antibodies. Secondary antibodies were a mixture of goat anti–rabbit IgG conjugated to 6-nm gold and donkey anti–guinea pig IgG tagged with 12-nm gold (Jackson ImmunoResearch Laboratories), each at 1:400 dilution.

For electron microscopy, the grids were stained with one drop of 5% uranyl acetate solution on parafilm for 10 min. After staining, the grids were immediately washed twice, each time for 10 min with a drop of double-distilled water. Excess water was removed from the grid by capillary action using 3MM paper (Whatman). The grids were air dried and examined in the Zeiss EM-10 operated at 80 kV.

Analysis of Gold Grain Distributions

To analyze the distribution of gold grains over the SC, electron micrographs were printed at a final magnification of 100,000. For each SC, the two lateral elements (defined by uranyl acetate staining) were traced on

each print. The distance from individual gold grains to the center of both lateral elements was measured using a digitizer (Bausch & Lomb). In addition, the width of the SC (i.e., distance between the center of the two lateral elements) was determined. The SC width deviates slightly from that of the mean value calculated for all sets of SCs sampled. This slight deviation was corrected by normalizing the width of each SC to the mean value of SC width. Finally, for analysis of the distribution of gold grains, the SC width was arbitrarily divided into 100 units, corresponding to ~1.1 nm for the wild-type SC and ~1.8 nm for the *zip1-3XH2* SC. The gold grain distribution was analyzed using StatView software (Abacus Concepts, Inc.).

To analyze the distribution of gold grains in polycomplexes and networks, the densely stained lines were traced on each print as described above for the lateral elements of the SC. The distances from individual gold grains to the center of the adjacent densely stained elements were determined. The distance between densely stained lines was also measured. The distribution of gold grains was analyzed as described for SCs.

Purification of Zip1 Proteins for In Vitro Assembly

To prepare Zip1 proteins for in vitro assembly, plasmids containing nearly full-length Zip1 as well as two truncated versions of Zip1, each tagged with 6xHis, were constructed in pQE30 (Qiagen) (see Fig. 1). pHD101 was made by cloning the BamHI-XbaI fragment from pTP29 (Tung and Roeder, 1998) into the BamHI and XbaI sites of pQE30. pHD115 was constructed by subcloning the HincII-PvuII fragment from pHD101 into the SmaI site of pQE30. Finally, pHD116 was made by isolating the BamHI-PvuII DNA fragment from pHD101 and ligating with pQE30 cleaved by BamHI and SmaI.

In plasmids pHD101, pHD115, and pHD116, the 6xHis-tagged Zip1 proteins are under the control of an inducible bacteriophage T5 promoter. For overexpression, plasmid-bearing cells of *E. coli* XL1-Blue were grown overnight at 37°C in 100 ml of LB medium (Sambrook et al., 1989) containing 200 μg/ml ampicillin. The overnight culture was diluted 1:20 into 1 liter of prewarmed LB medium containing 200 μg/ml ampicillin. The cells were grown at 37°C to an optical density at 600 nm of ~0.8, before induction with 1 mM isopropyl β-D-thiogalactopyranoside. After 3 h of induction, cells were pelleted at 4,000 *g* for 10 min and washed once in PBS buffer.

For purification of the 6xHis-Zip1 proteins, the cell pellet from 1 liter of culture was resuspended in 20 ml of lysis buffer (8 M urea, 0.1 M NaH_2PO_4, 2 mM EDTA, 10 mM Tris-Cl, pH 7.5). Cell lysis was achieved by rotating the cell suspension in lysis buffer for 60 min at room temperature. After centrifugation at 12,500 *g* for 10 min, the supernatant was mixed with 4 ml of 50% Ni-NTA resin (Qiagen) equilibrated in lysis buffer, and the resulting mixture was incubated for 30 min at 4°C. The protein bound Ni-NTA beads were washed with 50 ml of wash buffer A (8 M urea, 0.1 M NaH_2PO_4, 2 mM EDTA, 20 mM imidazole, 10 mM Tris-Cl, pH 6.2). Finally, the 6xHis-tagged Zip1 proteins were eluted in 1 ml of elution buffer A (8 M urea, 0.1 M NaH_2PO_4, 2 mM EDTA, 0.5 M imidazole, 10 mM Tris-Cl, pH 7.5).

The 6xHis-tagged Zip1 protein (specified by pHD101) was further purified by anion exchange chromatography to remove truncated polypeptides retaining the 6xHis tag. The 6xHis-Zip1 protein eluted from the Ni-NTA beads was desalted through the HiTrap desalting column (Pharmacia Biotech) in elution buffer B (6 M urea, 20 mM NaCl, 2 mM EDTA, 5 mM β-mercaptoethanol, 0.1 M Tris-Cl, pH 8.0) and immediately applied to an anion exchange HiTrap Q column (Pharmacia Biotech). Proteins were eluted using a linear salt gradient increasing from 10 mM to 1 M NaCl in elution buffer B. For further purification of the 6xHis-tagged Zip1-ΔC and Zip1-ΔNC proteins, the cation exchange HiTrap SP column (Pharmacia Biotech) was used. Elution of proteins from the HiTrap SP column was performed using a linear salt gradient from 10 mM to 1 M NaCl in the same buffer as for HiTrap Q except for 0.1 M Tris-Cl, pH 6.0. Fractions containing 6xHis-tagged proteins were analyzed on 8% SDS–polyacrylamide gels. Peak fractions containing Zip1 proteins were pooled, and protein concentrations were determined using the Bradford assay (Bio-Rad Laboratories).

In Vitro Assembly of Zip1

For in vitro assembly, purified Zip1 protein at a concentration of 0.5 mg/ml in 6 M urea was renatured by dialyzing the sample (1 ml) against a series of buffers (each 1 liter) with decreasing amounts of urea (6, 4, 2, and 1 M) in renaturation buffer (170 mM NaCl, 2 mM EDTA, 5 mM β-mercaptoethanol, 0.5 mM PMSF, 20 mM Tris-Cl, pH 8.0). After renaturation, the protein sample was dialyzed against dimerization buffer (20 mM triethanolamine, pH 8.0, 170 mM NaCl, 5 mM β-mercaptoethanol, 0.5 mM PMSF) for 4 h at 4°C. The protein sample was mixed with 10 μl of 20 mg/ml ethylene glycol bis (succinimidylsuccinate), a lysine-specific cross-linker (Geisler et al., 1983). Cross-linking was carried out for 30 min at 20°C. After quenching the reaction with 50 mM ethanolamine (pH 8.0) for 10 min on ice, the cross-linked sample was dialyzed against the dimerization buffer for 4 h to remove the cross-linker and ethanolamine.

The products formed in the cross-linking reaction were fractionated on a Superdex 200 gel filtration column (Pharmacia Biotech) mounted on a fast performance liquid chromatography system (Pharmacia Biotech). Gel filtration standards (Bio-Rad Laboratories) were run through the same column. Chromatography was performed at a flow rate of 1 ml/min in dimerization buffer and monitored with an ultraviolet monitor at 280 nm. Fractions of 1 ml were collected, and aliquots of each fraction were analyzed on 4–15% gradient SDS–polyacrylamide gels (Bio-Rad Laboratories) run at 100 V for 7 h.

Negative Staining and Electron Microscopy

Protein samples containing Zip1 dimers or tetramers at 100 μg/ml were diluted 1:10 and 1:50 with dimerization buffer. Aliquots (10 μl) of both the diluted and undiluted samples were deposited directly onto 200-mesh formvar/carbon–coated nickel grids (Electron Microscopy Sciences) that had been glow-discharged (Dodson and Echols, 1991). Excess liquid was removed from the grid by capillary action with 3MM paper (Whatman). Grids were air dried and stained with 3% uranyl acetate for 30 s. After removing excess uranyl acetate with 3MM paper, grids were air dried and examined at a magnification of 40,000 in a Zeiss EM-10 operated at 80 kV. Micrographs were taken at 100,000 magnification. For quantification of the length of Zip1 dimers, each micrograph was printed at a final magnification of 200,000, and rod length was measured using a digitizer.

Results

Preparation of Domain-specific Anti–Zip1 Antibodies

To generate antibodies specific for the three domains of Zip1, DNA fragments encoding nonoverlapping regions of the Zip1 protein were fused in-frame to the *GST* gene in a bacterial expression vector (Fig. 1 B). The Zip1-N fusion protein contains 120 amino acids from the NH_2-terminal globular domain of Zip1; Zip1-C contains the last 51 amino acids of the protein. The Zip1-coil fusion protein contains 239 amino acids from the region of coiled coil plus 75 amino acids from the COOH-terminal globular domain. The GST-Zip1 fusion proteins were purified from *E. coli* and used to raise antibodies in rabbits; in addition, the Zip1-C fusion protein was used to immunize guinea pigs. The resulting antibodies were purified from sera by affinity chromatography.

The specificity of the purified antibodies for Zip1 was tested by labeling meiotic chromosomes that had been surface spread. Spread chromosomes from wild type and a *zip1* mutant were probed with each of the test antibodies, followed by incubation with an appropriate secondary antibody with a fluorescent tag (Sym et al., 1993). All four test antibodies localized continuously along the lengths of pachytene chromosomes from the wild type, but not to chromosomes from the *zip1* null mutant (data not shown). Furthermore, the staining pattern obtained for each of the antibodies was indistinguishable from that obtained with polyclonal antibodies raised against the COOH-terminal half of the Zip1 protein (Sym et al., 1993). Pachytene chromosomes from wild type were not stained by any of the preimmune sera.

The specificity of antibodies for the different domains of Zip1 was determined by Western blot analysis. Aliquots of

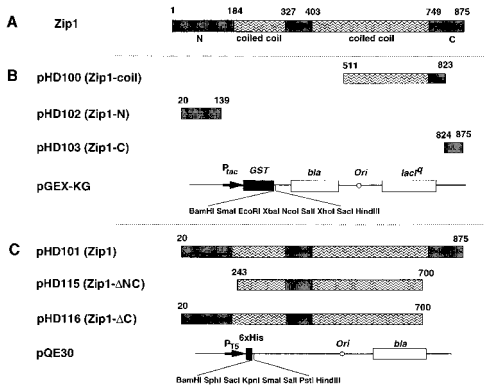

Figure 1. Plasmid constructions. (A) The three distinct domains of Zip1 are depicted schematically; the central coiled-coil region is predicted to contain a non–α-helical linker. (B) Plasmids used for preparation of anti–Zip1 antibodies. (C) Plasmids used to produce Zip1 for in vitro assembly reactions. Different segments of the *ZIP1* gene, identified by numbers corresponding to amino acid residues, were subcloned into the polylinker region in pGEX-KG (B) or pQE30 (C). N, NH_2-terminal domain of Zip1; C, COOH-terminal domain of Zip1; *GST*, glutathione-S-transferase gene; 6xHis, a hexamer of histidine residues; *bla*, ampicillin-resistance gene; *lacI*^{q}, a mutant version of the *lac* repressor; *Ori*, origin of plasmid DNA replication; P_{tac}, bacterial *tac* promoter; and P_{T5}, bacteriophage T5 promoter.

the three purified GST-Zip1 fusion proteins were fractionated by SDS-PAGE, blotted to nitrocellulose filters, and then probed with anti–Zip1-N, anti–Zip1-C and anti–Zip1-coil antibodies. As shown in Fig. 2, each of the three rabbit antibodies specifically recognizes the particular domain of Zip1 against which it was raised.

Organization of Zip1 within the SC

To determine the organization of the Zip1 protein within the central region of the SC, each of the three structural domains was mapped by immunogold labeling. The resolution of labeling was improved by using a mutant (*zip1-3XH2*) in which the width of the SC is increased ~1.7-fold compared with wild type (because of triplication of a restriction fragment encoding part of the coiled-coil region) (Sym and Roeder, 1995). Pachytene chromosomes prepared from a yeast strain overproducing the Zip1-3XH2 protein were spread on plastic-coated glass slides, and then incubated with DNase I to enhance the accessibility of SC antigens to anti–Zip1 antibodies. For immunogold labeling, plastic films containing meiotic chromosomes

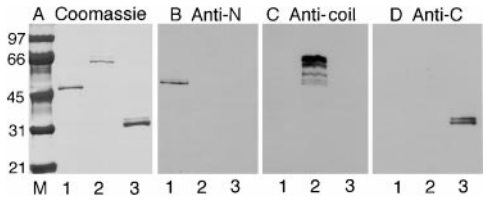

Figure 2. Western blot analysis of antibody specificity. The specificity of antibodies raised against three different fragments of Zip1 was examined by Western blot analysis. (A) 12% SDS–polyacrylamide gel stained with Coomassie brilliant blue showing the three GST-Zip1 fusion proteins used to raise antibodies. (lane 1) The NH_2-terminal domain–GST fusion (47 kD) encoded by pHD102; (lane 2) the coiled coil–GST fusion (62 kD) encoded by pHD100; and (lane 3) the COOH-terminal domain–GST fusion (32 kD) encoded by pHD103. The sizes of molecular weight markers (M) are indicated in kilodaltons on the left. (B–D) Western blots of the same Zip1 fusion proteins shown in A probed with anti–Zip1-N, anti–Zip1-coil, and anti–Zip1-C antibodies, respectively. The presence of more than one band in each lane can be attributed to degradation of Zip1-GST fusion proteins.

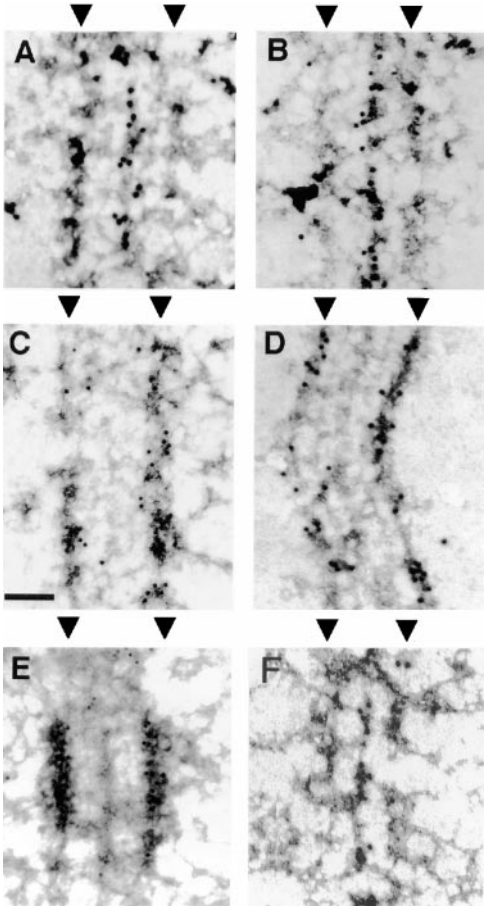

Figure 3. Electron micrographs of SCs labeled with gold-conjugated antibodies. SCs were probed first with primary antibodies specific for one of the three domains of Zip1, and then with a secondary antibody conjugated to colloidal gold as described in Materials and Methods. *zip1-3XH2* mutant SCs labeled with rabbit anti–Zip1-N (A and B) or anti–Zip1-C (C and D) antibodies. Secondary antibodies were tagged with 12-nm gold particles. The gold particles representing Zip1-N are concentrated in the middle region of the SC, whereas the gold particles representing Zip1-C are found over the lateral elements. (E) An SC from the *zip1-3XH2* mutant stained with rabbit antibodies to Zip1-N and guinea pig antibodies to Zip1-C. Anti–Zip1-N and anti–Zip1-C antibodies were detected with secondary antibodies tagged with 6- or 12-nm gold particles, respectively. The 12-nm gold (representing Zip1-C) is concentrated over the lateral elements, whereas the 6-nm gold (representing Zip1-N) localizes to the central element. (F) SC from wild type stained with anti–Zip1-N antibodies detected with secondary antibodies tagged to 12-nm gold particles. Antibodies localize to the central element. Arrowheads point to lateral elements. Bar, 100 nm.

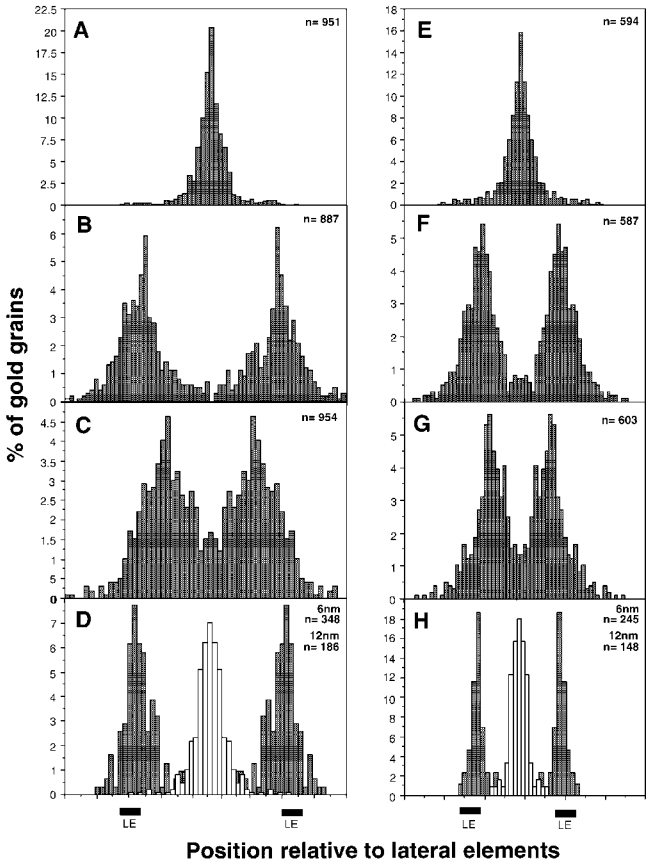

Figure 4. Distribution of gold grains over the SC. The distribution of gold grains over the SC was analyzed as described in Materials and Methods. The fraction of gold grains sampled was plotted as a function of position relative to lateral elements. The black bars at the bottom of each histogram represent the lateral elements of the SC. The number (n) of gold grains sampled is indicated in each graph. (A–D) Results obtained from the *zip1-3XH2* mutant SC; and (E–H) results derived from wild type. Shown are the distributions of gold grains obtained with anti–Zip1-N (A and E), anti–Zip1-C (B and F), and anti–Zip1-coil (C and G) antibodies. The gold grain distribution obtained from double labeling with rabbit anti–Zip1-N (open bars) and guinea pig anti–Zip1-C (filled bars) antibodies are shown in D and H.

were transferred to nickel grids that were subsequently probed with one of the three anti–Zip1 antibodies, followed by incubation with a secondary antibody conjugated to 12-nm gold particles. After staining with uranyl acetate, grids were examined in the EM and SCs were photographed (Fig. 3).

To analyze the distribution of gold grains over the SC, the distance from each gold grain to the center of each lateral element was measured, and the distribution of gold grains was plotted as a function of position relative to the lateral elements (Fig. 4). When the SC was probed with anti–Zip1-N antibodies, the majority of gold grains was located in the middle of the central region of the SC (Fig. 3, A and B, and Fig. 4 A). In cases where the central element was well defined by staining with uranyl acetate, the gold grains corresponding to the anti–Zip1-N antibody usually overlapped with the central element (Fig. 3, A and B). In contrast, when the SC was labeled with anti–Zip1-C antibodies, most of the gold grains were associated with the lateral elements (Fig. 3, C and D, and Fig. 4 B). Labeling of the SC with anti–Zip1-coil antibodies resulted in gold grains distributed throughout the central region, but concentrated midway between the central and lateral elements (Fig. 4 C).

Table I. Distances between Lateral Elements of SCs and Densely Stained Lines in Polycomplexes and Networks

	No. of heptad repeats	Predicted Zip1 dimer length	Observed distance	No. of measurements
		nm	*nm*	
SC (wild-type)	58	60	110 ± 9	387
SC (*zip1-3XH2*)	98	100	180 ± 11	204
Polycomplexes (*zip1-3XH2*)	98	100	178 ± 7	45
Networks (*zip1-3XH2*)	98	100	89 ± 6	51

Proteins capable of forming coiled coils consist of a seven-residue heptad repeat, in which the first and fourth amino acids are generally apolar. The distances between lateral elements of the SC as well as between two adjacent densely stained lines in polycomplexes and networks were measured after staining with uranyl acetate. Shown are the mean values with SDs.

Double labeling experiments were also performed on SCs from the *zip1-3XH2* mutant. In this experiment, meiotic chromosome spreads were probed simultaneously with rabbit anti–Zip1-N and guinea pig anti–Zip1-C antibodies, followed by incubation with a mixture of anti-rabbit IgG conjugated with 6-nm gold particles and anti–guinea pig IgG conjugated with 12-nm colloidal gold. As shown in Figs. 3 E and 4 D, the smaller 6-nm gold grains lie in the middle of the central region, whereas the larger 12-nm gold particles are associated with the lateral elements.

To confirm these results for wild-type SCs, meiotic chromosomes prepared from a wild-type strain were used for immunogold labeling. As expected, the width of the wild-type SC (~110 nm) is significantly narrower than that of the mutant SC (~180 nm), as determined by uranyl acetate staining (Table I). However, the distribution of gold grains in the wild-type SC is similar to that in the mutant SC for each of the domain-specific anti–Zip1 antibodies (Fig. 3 F and Fig. 4, E–H). These results suggest that the NH_2-terminal domain of Zip1 lies in the central element, whereas the COOH-terminal domain is anchored in the lateral elements such that two Zip1 dimers, lying head-to-head, span the width of the SC.

Organization of Zip1 in Polycomplexes and Networks

Overproduction of the Zip1 protein results in the formation of two highly ordered nuclear structures called polycomplexes and networks (Sym and Roeder, 1995). Both structures contain the Zip1 protein and are unassociated with chromatin. Elucidating the organization of Zip1 in polycomplexes and networks may provide insight into the polymerization of Zip1. Polycomplexes and networks stained by uranyl acetate (Fig. 5, A and B) are structurally similar to those observed after staining with silver nitrate (Sym and Roeder, 1995).

Polycomplexes consist of a number of densely stained lines stacked in parallel (Fig. 5 A). In both wild type and the *zip1-3XH2* mutant, the distance between these lateral

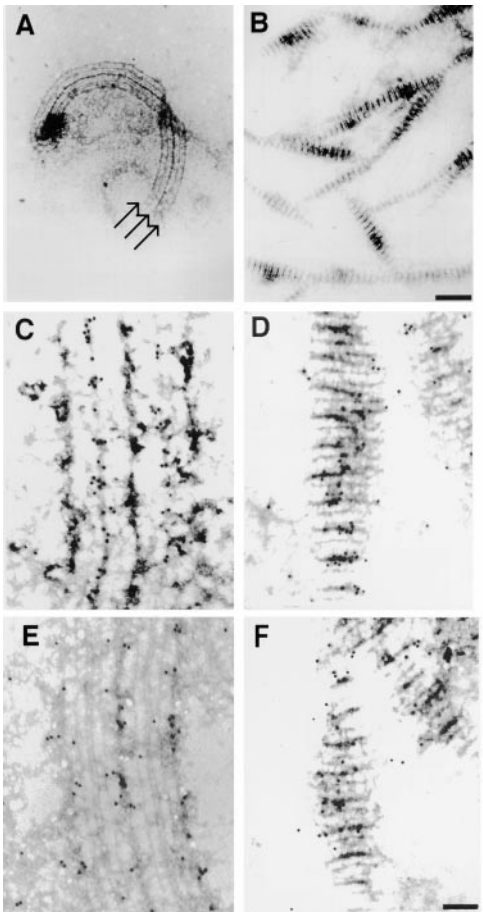

Figure 5. Electron micrographs of polycomplexes and networks labeled with gold-conjugated antibodies. The overall structures of polycomplexes and networks (from the *zip1-3XH2* mutant) stained by uranyl acetate are shown in A and B, respectively. The arrows in A indicate lateral element-like structures. (C and E) Segments of polycomplexes labeled with anti–Zip1-N and anti–Zip1-C antibodies, respectively. Anti–Zip1-N antibodies are concentrated over the central element-like structures, which stain less intensely with uranyl acetate. Anti–Zip1-C antibodies localize to the lateral element-like structures, which are more intensely staining. (D and F) Segments of networks labeled with anti–Zip1-N and anti–Zip1-C antibodies, respectively. Antibodies to both Zip1-N and Zip1-C are concentrated over the elements that stain intensely with uranyl acetate; these alternate with parallel lines that are lightly stained. Bars: (A and B) 500 nm; (C–F) 100 nm.

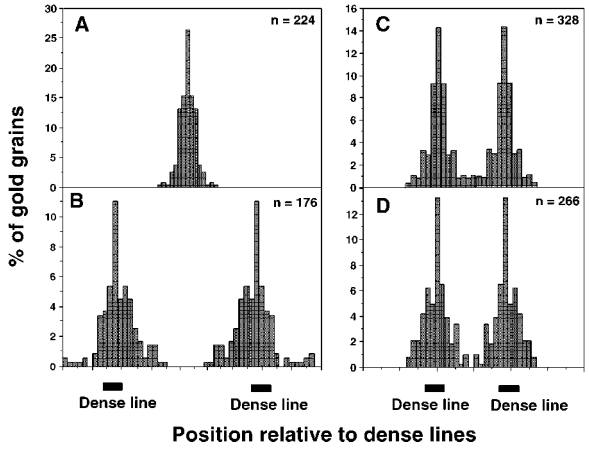

Figure 6. Distribution of gold grains within polycomplexes and networks. Shown are the distributions of gold grains for polycomplexes (A and B) and networks (C and D) labeled with anti–Zip1-N (A and C) and anti–Zip1-C (B and D) antibodies. The black bars at the bottom of the histograms correspond to the densely stained lines in polycomplexes and networks; the distance between two adjacent dense lines in polycomplexes is twice that in networks.

element-like structures corresponds to the distance between lateral elements in mature SCs (Sym and Roeder, 1995; Table I). A lightly stained element (presumably analogous to the central element) runs equidistant between each pair of darkly stained lines. To define the organization of Zip1 in polycomplexes, immunogold labeling was performed on polycomplexes derived from yeast overproducing the Zip1-3XH2 protein. The densely stained lines were used as references from which to measure the distance to each gold grain, and the distribution of gold grains relative to the darkly stained elements was plotted (Fig. 6). When polycomplexes were probed with anti–Zip1-N antibody, most of the gold grains were found in the middle of the spaces between densely stained lines (Figs. 5 C and 6 A). Furthermore, these gold grains appeared to coincide with the lightly stained elements (i.e., the structures presumably analogous to the central element). In contrast, anti–Zip1-C antibodies specifically labeled the densely stained elements (Figs. 5 E and 6 B).

Networks consist of multiple parallel lines arranged into a complex array that branches out in several different directions (Fig. 5 B). A lightly stained line is also discernible between adjacent darkly stained elements in networks, but this line is slightly off center relative to the flanking elements. Whereas the average distance between two densely stained lines in polycomplexes approximates the width of the SC, the average distance between darkly stained lines in networks corresponds to roughly half the width of the SC (Table I). Immunogold labeling of networks revealed that the densely stained elements are labeled with gold grains regardless of whether anti–Zip1-N or anti–Zip1-C antibodies are used (Fig. 5, D and F, and Fig. 6, C and D). These data indicate that the structural organization of Zip1 in networks is fundamentally different from that in SCs and polycomplexes.

Purified Zip1 Proteins Form Dimers and Tetramers In Vitro

The formation of highly ordered chromatin-free structures upon Zip1 overproduction (Sym and Roeder, 1995) suggests that the Zip1 protein has a capacity for self assembly. To test this idea, Zip1 protein was purified from bacteria and examined for the ability to form dimers and higher order multimers in vitro. Nearly full-length Zip1 protein, as well as two truncated versions of Zip1, were fused to a 6xHis tag in the vector pQE30 (Fig. 1 C). One truncated version of Zip1 is devoid of the COOH-terminal domain (Zip1-CΔ), whereas the other lacks both the NH_2- and

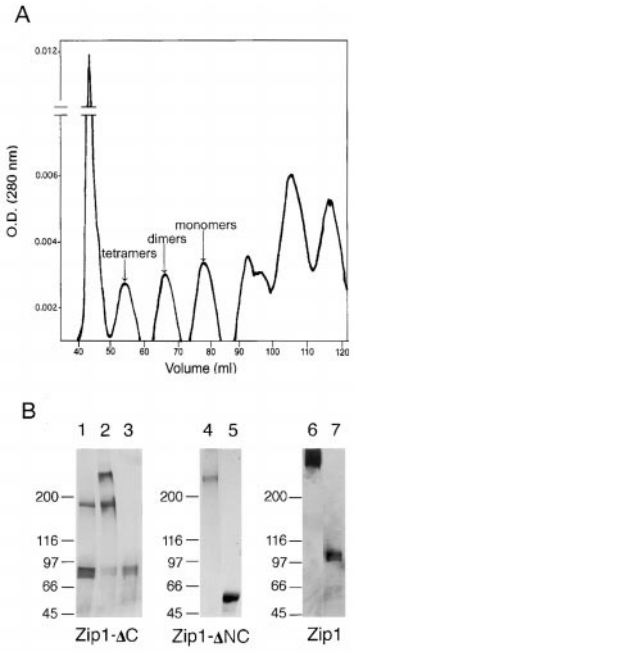

Figure 7. Fractionation and analysis of Zip1 dimers and tetramers. The products of Zip1 assembly in vitro were fractionated by gel filtration and analyzed on an SDS–polyacrylamide gel. (A) Gel filtration profile of the Zip1-ΔC protein. The peaks presumed to correspond to monomers, dimers, tetramers, and higher order oligomers are indicated. (B) SDS-PAGE analysis of Zip1 monomers, dimers, and tetramers. Shown are samples of Zip1-ΔC dimers (lane 1), tetramers (2) and monomers (3), Zip1-ΔNC tetramers (4) and monomers (5), and wild-type tetramers (6) and monomers (7). The dimer and tetramer samples represent fractions derived from gel filtration; Zip1 monomers (Zip1-ΔC, 78 kD; Zip1-ΔNC, 48 kD; and Zip1, 100 kD) are protein samples before incubation in polymerization buffer and cross-linking. The sizes of molecular weight markers are indicated in kilodaltons to the left of each panel.

COOH-terminal domains (Zip1-ΔNC) (Fig. 1 C). The 6xHis-Zip1 proteins were overproduced in bacteria, and then purified by nickel chromatography.

For in vitro assembly, purified and denatured Zip1 protein was gradually transferred to conditions suitable for renaturation. After stabilization with a lysine-specific cross-linker, the products of renaturation were fractionated by gel filtration using a Superdex 200 column. The elution profile for the Zip1-ΔC protein reveals several peaks, with molecular weights suggestive of monomers, dimers, tetramers, and higher order oligomers (Fig. 7 A). When fractions presumed to correspond to dimers were analyzed by SDS-PAGE, both dimers and monomers were detected (Fig. 7 B). Electrophoretic analysis of fractions presumed to contain tetramers revealed a mixture of tetramers, dimers, and monomers (Fig. 7 B). (The presence of monomers in the dimer fraction, and of dimers and monomers in the tetramer fraction, suggests that cross-linking was incomplete.) In contrast, when the nearly full-length Zip1 protein and the Zip1-ΔNC protein were analyzed by gel filtration, only peaks corresponding to tetramers and higher order multimers were observed (data not shown).

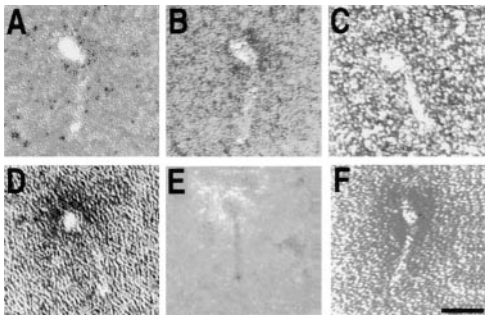

Figure 8. Electron micrographs of Zip1-ΔC dimers. Protein samples containing fractionated Zip1 dimers were deposited onto EM grids and negatively stained with uranyl acetate. Bar, 50 nm.

These results indicate that Zip1 is capable of forming dimers and tetramers in vitro. In the case of the nearly full-length and Zip1-ΔNC proteins, the tetramer appears to be the predominant form resulting from in vitro assembly; presumably, dimers are formed in vitro, but these are rapidly converted into tetramers.

Electron Microscopic Visualization of Zip1 Dimers

To determine the configuration of Zip1 monomers within dimers, the dimer fraction derived from gel filtration of the Zip1-ΔC protein was spotted on formvar/carbon–coated EM grids that had been glow discharged. After negative staining with uranyl acetate, grids were examined in the EM. If two Zip1-ΔC molecules form a dimer in which the two monomers are in the same orientation and in register, then a dimer should appear as a rod-shaped structure with a globular domain (or domains) at only one end. An antiparallel configuration would produce a rod-shaped dimer with a globular domain at each end. As shown in Fig. 8, each Zip1-ΔC dimer appears as a globular domain attached to a rod-shaped structure. In addition, some globular molecules were observed, presumably representing monomers; however, there were no obvious rod-shaped molecules without a globular domain at one end, rods with globular domains at both ends, or rod-shaped structures with a globular domain in the middle. The average length of the rod domain in the Zip1-ΔC dimer (51.2 + 2.7 nm, based on 48 measurements) is similar to the value predicted (51.9 nm) based on the number of heptad repeats (50) in the Zip1-ΔC protein. These observations suggest that two monomers in a Zip1 dimer are arranged in parallel and in register.

Attempts to determine the organization of dimers within tetramers were confounded by the tendency of these molecules to aggregate into disorganized higher order oligomers before or during the transfer to EM grids (data not shown).

Discussion

Zip1 Forms a Coiled-Coil Homodimer

Based on its amino acid sequence, the Zip1 protein is predicted to form a coiled coil in which two molecules wrap around a common axis to form an extended, rod-shaped

dimer (Cohen and Parry, 1986). Thus, it is generally assumed that Zip1 (and its mammalian counterparts, SCP1/Syn1) form homodimers, analogous to myosin and most intermediate filament proteins (Fuchs and Weber, 1994). However, this has not been directly demonstrated for any SC protein. These proteins might fail to form rod-shaped molecules, or they might associate with another (as yet unidentified) protein to form a heterodimer, as is the case for the keratin family of intermediate filament proteins (Fuchs and Weber, 1994). We have purified the Zip1 protein from bacteria and visualized the products of in vitro assembly in the EM. This analysis demonstrates that two Zip1 monomers associate to form a dimer with a rod-shaped domain of the length predicted if the two protein chains are in register with each other. The Zip1-ΔC protein forms a dimer with a head domain at one end of the rod, indicating that the monomers are oriented in parallel, as is the case for other coiled-coil proteins (Fuchs and Weber, 1994). The failure to observe two distinct globular domains at the end of the rod may indicate that the NH_2 termini of the two Zip1 monomers within the dimer interact with each other. In this regard, it is of interest that the NH_2 terminus of the mouse SCP1 protein has been demonstrated to interact with itself in the two-hybrid protein system (Liu et al., 1996).

Two Zip1 Dimers, Lying Head-to-Head, Span the Width of the SC

Immunogold labeling of the SC with domain-specific Zip1 antibodies indicates that the NH_2-terminal domain of Zip1 lies in the central element of the SC, whereas the COOH-terminal domain is embedded in a lateral element. This arrangement is consistent with previous studies demonstrating that sequences in the Zip1 COOH terminus (amino acids 800–824) are specifically required for its localization to chromosomes (Tung and Roeder, 1998). Transverse filaments that span the full width of the SC central region would consist of two Zip1 dimers, lying head-to-head (Fig. 9 A). Filaments that pass half way through the SC, bridging the space between one lateral element and the central element, would consist of a Zip1 dimer anchored to a single lateral element (Fig. 9 A).

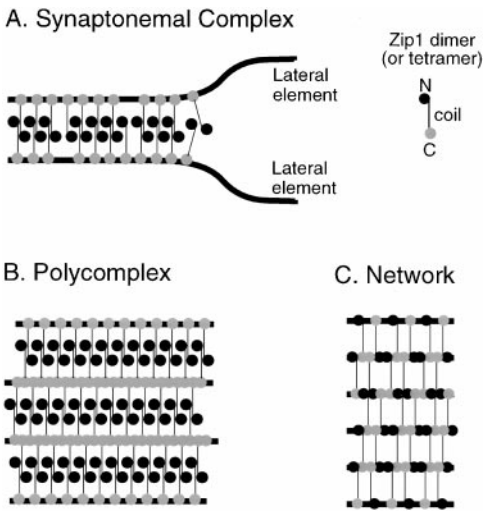

Figure 9. Models for the organization of Zip1 in the SC, polycomplexes, and networks. (A) Organization of Zip1 in the SC. Two Zip1 dimers, lying head-to-head, span the entire width of the SC. It is possible that the basic building block of the SC central region is a tetramer, consisting of two dimers lined up side-by-side, in parallel, and in register. (B) Arrangement of Zip1 in polycomplexes. As in SCs, two Zip1 dimers, lying head-to-head, bridge the space between two densely stained lines. (C) Organization of Zip1 in networks. Individual Zip1 dimers connect the two dense lines in both possible orientations.

Ultrastructural studies of SCs in rodents and insects have shown that transverse filaments range in diameter from 2 to 10 nm (Wettstein and Sotelo, 1971; Solari and Moses, 1973; Schmekel et al., 1993b). Individual transverse filaments often appear to be split into two or more thinner fibers, with this splitting particularly apparent just inside the lateral elements (Wettstein and Sotelo, 1971; Schmekel et al., 1993b). These observations suggest that transverse filaments consist of bundles of thin fibers, with the elementary fiber being ~2 nm in diameter. This is the diameter expected for the rod-shaped region of a coiled-coil protein (Fuchs and Weber, 1994). Thus, a variable number of Zip1 dimers may bundle together to form a transverse filament.

The results of gel filtration suggest that two Zip1 dimers tend to associate with each other to form homotetramers. If such tetramers are intermediates in SC assembly in vivo, they could exist in either of two forms. The two dimers could be arranged head-to-head and in an antiparallel orientation, analogous to a transverse filament that spans the full width of the SC. Alternatively, the two dimers within a tetramer could lie side-by-side and in parallel, analogous to a transverse filament that spans half the width of the SC. The ability of the Zip1-ΔNC protein to form tetramers in vitro suggests that the globular domains at the ends of the Zip1 protein are not required for tetramer formation and is most consistent with a side-by-side alignment of dimers to form tetramers. Therefore, we suspect that two Zip1 dimers bundle together to form a tetramer, and this tetramer serves as the basic building block of the SC central region. Tetramers would associate with axial elements first, and then interact (directly or indirectly) to form an octamer that spans the width of the SC (Fig. 9 A).

If two Zip1 dimers (or dimer bundles) span the width of the SC, what holds these molecules together in the middle of the central region? An obvious possibility is that the NH_2 termini of Zip1 dimers attached to paired lateral elements interact with each other, as proposed for SCP1 (Liu et al., 1996). However, analysis of in-frame deletion mutants of Zip1 has shown that the NH_2-terminal globular domain of Zip1 is not essential for synapsis (Tung and Roeder, 1998). Another possibility is that the two Zip1 dimers associated with parallel lateral elements partially overlap in the region of coiled coil (Fig. 9 A), as suggested previously (Tung and Roeder, 1998). Thus, interactions between coiled-coil segments immediately proximal to the NH_2 terminus might hold Zip1 dimers together. This hypothesis is consistent with the observation that a mutant (Zip1-M1) lacking amino acids 244–511 of the coiled coil fails to make SC (or makes SCs that are extremely unstable) even though the Zip1 protein does localize along the lengths of paired axial elements (Tung and Roeder, 1998).

A third possibility is that Zip1 dimers attached to paired lateral elements are held together by another (unknown) protein that interacts with the coiled-coil domains of the two dimers and serves as a bridge between them. In this case, the Zip1-M1 mutant may be missing the region of interaction with this linker protein.

In studies of SC ultrastructure, the central element of the complex displays a characteristic ladderlike appearance (Wettstein and Sotelo, 1971; Solari and Moses, 1973; Schmekel et al., 1993a,b; Schmekel and Daneholt, 1995). Two parallel elements run longitudinally and are connected by regularly spaced transverse fibers. The transverse filaments of the SC appear to pass through (and perhaps form) the rungs of the ladder. It has been suggested that the longitudinal components of the central element correspond to the NH_2 termini of coiled-coil proteins such as SCP1/Syn1/Zip1 (Liu et al., 1996). Two rows of NH_2-terminal globular domains could appear as thin longitudinal structures at the outer edges of the central element (Fig. 9 A). The transverse components of the central element appear thicker than the transverse filaments outside the central element (Schmekel and Daneholt, 1995), perhaps because there are twice as many coiled coils within the central element compared with the regions flanking this element (Fig. 9 A).

Zip1 Is Organized Differently in Polycomplexes and Networks

Overproduction of the Zip1 protein results in the production of polycomplexes and networks, both of which are unassociated with chromosomal DNA. Polycomplexes have been observed during meiosis in wild-type yeast (though not in the strain background used for these experiments); however, networks have been observed only under conditions of Zip1 overproduction. Polycomplexes have also been observed in a wide variety of plants and animals (e.g., Fiil and Moens, 1973; Bogdanov, 1977; Esponda and Krimer, 1979; Stack and Roelofs, 1996) where they are most often found during or after the pachytene stage (for review see Goldstein, 1987). The organization of Zip1 in polycomplexes is consistent with the long-standing assumption that these complexes represent multiple SC-like structures stacked in parallel. In SCs and in polycomplexes, two Zip1 dimers, lying head-to-head, span the distance between lateral elements and densely stained lines, respectively (Fig. 9, A and B). In contrast, in networks, a single Zip1 dimer spans the space between two densely stained lines and can lie in both possible orientations (Fig. 9 C). Nuclei from cells overproducing Zip1 contain either a polycomplex or a network, but never both. This observation suggests that nucleation of these structures is rate limiting, and that once a particular structure is initiated, the organization of Zip1 is determined and subsequently propagated.

Polycomplexes resulting from Zip1 overproduction are often elongate structures in which two to four SCs appear to be stacked in parallel and extend for a considerable distance in a direction perpendicular to the axis of the Zip1 dimer (Sym and Roeder, 1995). This suggests that once a polycomplex has been nucleated, its subsequent elongation is mechanistically related to SC assembly. In both cases, side-by-side associations between parallel Zip1 dimers (or tetramers) could be the driving force. In contrast, networks are extended in a direction parallel to the axis of the Zip1 dimer, as if polymerization of these structures is due to head-to-head, tail-to-tail, and/or head-to-tail interactions between dimers. In these unusual structures, the affinity between Zip1 dimers lying side-by-side appears to be reduced, as suggested by the narrow width of networks and the tendency of these structures to split into separate branches. The affinity between two Zip1 dimers lying side-by-side in antiparallel orientation may be lower than that between two parallel side-by-side dimers.

Three-dimensional analysis of SCs by EM tomography has revealed that the central region of the SC from insects and rodents is multilayered, with three to four transverse filaments and central elements stacked one on top of each other (Schmekel et al., 1993a,b). Thin section analysis of yeast SCs, however, suggests that these structures are a single layer in depth (Byers and Goetsch, 1975). Nevertheless, it is possible that networks and/or polycomplexes consist of multiple layers. In particular, variations in depth may account for the observed variability in the staining intensity of networks at different positions throughout the branched array. The most densely stained segments may correspond to regions in which multiple Zip1 dimers are stacked on top of each other.

In favorable preparations of *zip1-3XH2* polycomplexes stained with uranyl acetate (Fig. 5 E), detailed substructure is apparent in the central region. The central element can be clearly seen to consist of two parallel lines (the side pieces of the ladder referred to above). In addition, a very lightly stained line runs parallel to and equidistant between the lines presumed to correspond to lateral and central elements. These faint lines may correspond to the interruption in the Zip1 coiled coil; if this linker region (Fig. 1 A) folds into a small globular domain, then juxtaposition of these globes might create the appearance of a continuous line.

The Organization of Zip1 Is Similar to that of SCP1/Syn1

As noted in the Introduction, the Zip1 protein is structurally similar to the SCP1 protein of rats and its homologues in humans, mice, and hamsters. Each of these proteins is predicted to form a rod-shaped coiled-coil domain flanked by globular domains, and each protein localizes specifically to the central region of synapsed meiotic chromosomes. The predicted amino acid sequences for the mammalian proteins are 74–93% identical to each other, and homology extends along the entire length of these proteins (Meuwissen et al., 1992, 1997; Dobson et al., 1994; Sage et al., 1995; Liu et al., 1996). In contrast, the homology between Zip1 and the mammalian proteins does not extend outside the region of coiled coil. Furthermore, within the region of a predicted coiled coil, the homology is no greater than expected for any two proteins that form amphipathic α-helices.

Given the lack of significant sequence similarity between Zip1 and SCP1/Syn1, it is perhaps surprising to discover that these proteins are similarly organized within the

central region of the SC. Epitope mapping experiments involving the rat, mouse, and hamster proteins indicate that the COOH termini are embedded in lateral elements, whereas the NH_2 termini protrude into the middle of the central region of the SC (Dobson et al., 1994; Liu et al., 1996; Schmekel et al., 1996). Thus, as is the case for Zip1, two head-to-head dimers in antiparallel orientation span the width of the SC. These results suggest that Zip1 is both a structural and functional homologue of SCP1/Syn1 and raise the intriguing question of whether the genes encoding Zip1 and SCP1/Syn1 arose independently during evolution or diverged from a common ancestor. In this regard, it is noteworthy that there is no homologue of SCP1/Syn1 in the yeast genome, and there is no homologue of Zip1 or SCP1/Syn1 in the *C. elegans* genome. The lack of sequence similarity for a major structural component of the SC is surprising, considering the striking morphological similarities among SCs from different species (von Wettstein et al., 1984).

We thank Seema Agarwal, Jennifer Fung, Janet Novak, Beth Rockmill and Pedro San-Segundo for valuable comments on the manuscript. We are grateful to Kimberly Owens for assistance in manuscript preparation. We also thank Barry Piekos for technical assistance in electron microscopy (all individuals from Yale University, New Haven, CT).

This project was supported by the National Institutes of Health grant GM28904 to G.S. Roeder and by the Howard Hughes Medical Institute.

Submitted: 27 August 1999
Revised: 21 December 1999
Accepted: 23 December 1999

References

Bogdanov, Y.F. 1977. Formation of cytoplasmic synaptonemal-like polycomplexes at leptotene and normal synaptonemal complexes at zygotene in *Ascaris summ* male meiosis. *Chromosoma*. 61:1–21.

Byers, B., and L. Goetsch. 1975. Electron microscopic observations on the meiotic karyotype of diploid and tetraploid *Saccharomyces cerevisiae*. *Proc. Natl. Acad. Sci. USA*. 72:5056–5060.

Cohen, C., and D.A. Parry. 1986. α-Helical coiled coils: a widespread motif in proteins. *Trends Biochem. Sci.* 11:245–248.

Dobson, M.J., R.E. Pearlman, A. Karaiskakis, B. Spyropoulos, and P.B. Moens. 1994. Synaptonemal complex proteins: occurrence, epitope mapping and chromosome disjunction. *J. Cell Sci.* 107:2749–2760.

Dodson, M., and H. Echols. 1991. Electron microscopy of protein-DNA complexes. *Methods Enzymol.* 208:168–196.

Esponda, P., and D.B. Krimer. 1979. Development of the synaptonemal complex and polycomplex formation in three species of grasshoppers. *Chromosoma*. 73:237–245.

Fiil, A., and P.B. Moens. 1973. The development, structure and function of modified synaptonemal complexes in mosquito oocytes. *Chromosoma*. 41: 37–62.

Fuchs, E., and K. Weber. 1994. Intermediate filaments: structure, dynamics, function, and disease. *Annu. Rev. Biochem*. 63:345–382.

Geisler, N., E. Kaufmann, S. Fischer, U. Plessmann, and K. Weber. 1983. Neurofilament architecture combines structural principles of intermediate filaments with carboxy-terminal extensions increasing in size between triplet proteins. *EMBO (Eur. Mol. Biol. Organ.) J.* 2:1295–1302.

Goldstein, P. 1987. Multiple synaptonemal complexes (polycomplexes): origin, structure and function. *Cell Biol. Int. Rep.* 11:759–796.

Guan, K., and J.E. Dixon. 1991. Eukaryotic proteins expressed in *Escherichia coli*: an improved thrombin cleavage and purification procedure of fusion proteins with glutathione S-transferase. *Anal. Biochem*. 192:262–267.

Heyting, C. 1996. Synaptonemal complexes: structure and function. *Curr. Opin. Cell Biol.* 8:389–396.

Liu, J.-G., L. Yuan, E. Brundell, B. Bjorkroth, B. Daneholt, and C. Hoog. 1996. Localization of the N-terminus of SCP1 to the central element of the synaptonemal complex and evidence for direct interactions between the N-termini of SCP1 molecules organized head-to-head. *Exp. Cell Res.* 226:11–19.

Lupas, A., M.V. Dyke, and J. Stock. 1991. Predicting coiled-coils from protein sequences. *Science*. 252:1162–1164.

Meuwissen, R.L.J., H.H. Offenberg, A.J.J. Dietrich, A. Riesewijk, M.V. Iersel, and C. Heyting. 1992. A coiled-coil related protein specific for synapsed regions of meiotic prophase chromosomes. *EMBO (Eur. Mol. Biol. Organ.) J.* 11:5091–5100.

Meuwissen, R.L.J., I. Meerts, J.M.N. Hoovers, N.J. Leschot, and C. Heyting. 1997. Human synaptonemal complex protein 1 (SCP1): isolation and characterization of the cDNA and chromosomal localization of the gene. *Genomics*. 39:377–384.

Rockmill, B., and G.S. Roeder. 1990. Meiosis in asynaptic yeast. *Genetics*. 126: 563–574.

Roeder, G.S. 1997. Meiotic chromosomes: it takes two to tango. *Genes Dev*. 11: 2600–2621.

Sage, J., L. Martin, F. Cuzin, and M. Rassoulzadegan. 1995. cDNA sequence of the murine synaptonemal complex protein 1 (SCP1). *Biochim. Biophys. Acta*. 1263:258–260.

Sambrook, J., E.F. Fritsch, and T. Maniatis. 1989. Molecular Cloning: A Laboratory Manual. Cold Spring Harbor Laboratory, Cold Spring Harbor, New York.

Schmekel, K., and B. Daneholt. 1995. The central region of the synaptonemal complex revealed in three dimensions. *Trends Cell Biol.* 5:239–242.

Schmekel, K., U. Skoglund, and B. Daneholt. 1993a. The three-dimensional structure of the central region in a synaptonemal complex: a comparison between rat and two insect species, *Drosophila melanogaster* and *Blaps cribosa*. *Chromosoma*. 102:682–692.

Schmekel, K., J. Wahrman, U. Skoglund, and B. Daneholt. 1993b. The central region of the synaptonemal complex in *Blaps cribosa* studied by electron microscope tomography. *Chromosoma*. 102:669–681.

Schmekel, K., R.L.J. Meuwissen, A.J.J. Dietrich, A.C.G. Vink, J. van Marle, H. van Veen, and C. Heyting. 1996. Organization of SCP1 protein molecules within synaptonemal complexes of the rat. *Exp. Cell Res.* 227:20–30.

Smith, A.V., and G.S. Roeder. 1997. The yeast Red1 protein localizes to the cores of meiotic chromosomes. *J. Cell Biol.* 136:957–967.

Solari, A.J., and M.J. Moses. 1973. The structure of the central region in the synaptonemal complexes of hamster and cricket spermatocytes. *J. Cell Biol.* 56:145–152.

Stack, S.M. and D. Roelofs. 1996. Localized chiasmata and meiotic nodules in the tetraploid onion *Allium porrum*. *Genome*. 39:770–783.

Steinert, P.M., and D.R. Roop. 1988. Molecular and cellular biology of intermediate filaments. *Annu. Rev. Biochem*. 57:593–625.

Sym, M., and G.S. Roeder. 1995. Zip1-induced changes in synaptonemal complex structure and polycomplex assembly. *J. Cell Biol.* 128:455–466.

Sym, M., J. Engebrecht, and G.S. Roeder. 1993. ZIP1 is a synaptonemal complex protein required for meiotic chromosome synapsis. *Cell*. 72:365–378.

Tung, K.-S., and G.S. Roeder. 1998. Meiotic chromosome morphology and behavior in *zip1* mutants of *Saccharomyces cerevisiae*. *Genetics*. 149:817–832.

von Wettstein, D., S.W. Rasmussen, and P.B. Holm. 1984. The synaptonemal complex in genetic segregation. *Annu. Rev. Genet.* 18:331–413.

Wettstein, R., and J.R. Sotelo. 1971. The molecular architecture of synaptonemal complexes. *In* Advances in Cell and Molecular Biology. Vol. 1. E.J. DuPraw, editor. Academic Press, New York. 109–152.